

1 **Modeling stand-level forest attributes using lidar and Common**

2 **Stand Exam data**

3

4

5

6 Brett L Lawrence ^{AB*}, +1-936-581-6833, lawrenceb3@jacks.sfasu.edu; coauthors

7 ^A Stephen F. Austin State University, 1936 North St, Nacogdoches, Texas 75962, USA

8 ^B Raven Environmental Services, Inc., 6 Oak Bend Drive, Huntsville, Texas 77340, USA

9 * Corresponding Author: lawrenceb3@jacks.sfasu.edu

10

11

12

13 This manuscript a non-peer reviewed preprint submitted to EarthArXiv. It has also been submitted to
14 scientific journal, and following peer-review will potentially undergo changes from its preprint
15 version.

16 **Abstract**

17 Traditional forest inventories provide important information to forest managers regarding stand
18 volume, structure, and species composition. While crucial for making informed decisions, forest
19 inventories can be time intensive, costly, and acquisition can delay forest management actions. In
20 some cases, publicly available and large-scale LiDAR datasets can serve as a means for assisting
21 with or even substituting for pedestrian methods when collecting forest inventory data. This study
22 focuses on the development of a new geospatial methodology and model development where LiDAR
23 data was leveraged to recreate Common Stand Exam (CSE) results. CSE protocols are the U.S.
24 Forest Service's approach to conducting forest inventories, with Live Tree Stocking and Volume
25 reports being major outputs following field data acquisition. Modelling efforts yielded statistically
26 significant similarities in BA, TPA, board-feet volume, and tonnage volume when comparing
27 traditionally acquired CSE data versus LiDAR-based analysis. While lidar-based approaches might
28 not be appropriate for every forest management objective, these results demonstrate that they have
29 the potential to be leveraged in scenarios where major forest metrics are required. This could
30 represent significant time and cost efficiency for forest managers who are confronted with
31 challenging deadlines, fiscal limitations, and harsh environmental conditions.

32 **Keywords:** lidar, Common Stand Exam, shortleaf pine, loblolly pine, forest inventory

33 **Introduction**

34 Stand-level forest attribute data is an important resource for managers when making decisions about
35 forest prescriptions and treatments. Forest management often happens at the stand-level or multi

36 stand-level scale but stand inventory and volume data are not always readily available. Its acquisition
37 can be cost and time-prohibitive, with timber cruises requiring significant personnel time in the field.

38 Alternatives that reduce or eliminate the need for personnel intensive field work have been applied
39 using a variety of methods (Hummel et al., 2011; Brosofske et al., 2014; Hemingway and Opalach,
40 2024). They typically involve the acquisition of some remote sensing dataset using spaceborne,
41 airborne, or UAV-borne methods, and analyzing that data to model forest attributes. When and where
42 these methods can be applied effectively is highly circumstantial, and depend on factors such as
43 resource availability, budget, and the spatial scale being assessed. For example, a UAV or drone
44 might be a cost-effective option for forest managers with limited resources and budget, but the spatial
45 scale they operate within is relatively small and inadequate for assessing larger areas.

46 Lidar is often the foundational remote sensing dataset used when recreating forest attributes that
47 characterize structure and species composition (Dubayah et al., 2000; Balestra et al., 2024). Lidar
48 data is comprised of laser pulses from the sensor, or returns, that measure the heights of vegetation
49 and physical features on some terrestrial surface. The resulting point cloud datasets can vary in
50 density and are capable of modeling forest vegetation in precise detail (Sumnall et al., 2021; Ross et
51 al., 2024). This includes modeling species richness and composition of forests using lidar-derived
52 explanatory metrics (Anderson et al., 2021; Wu et al., 2024).

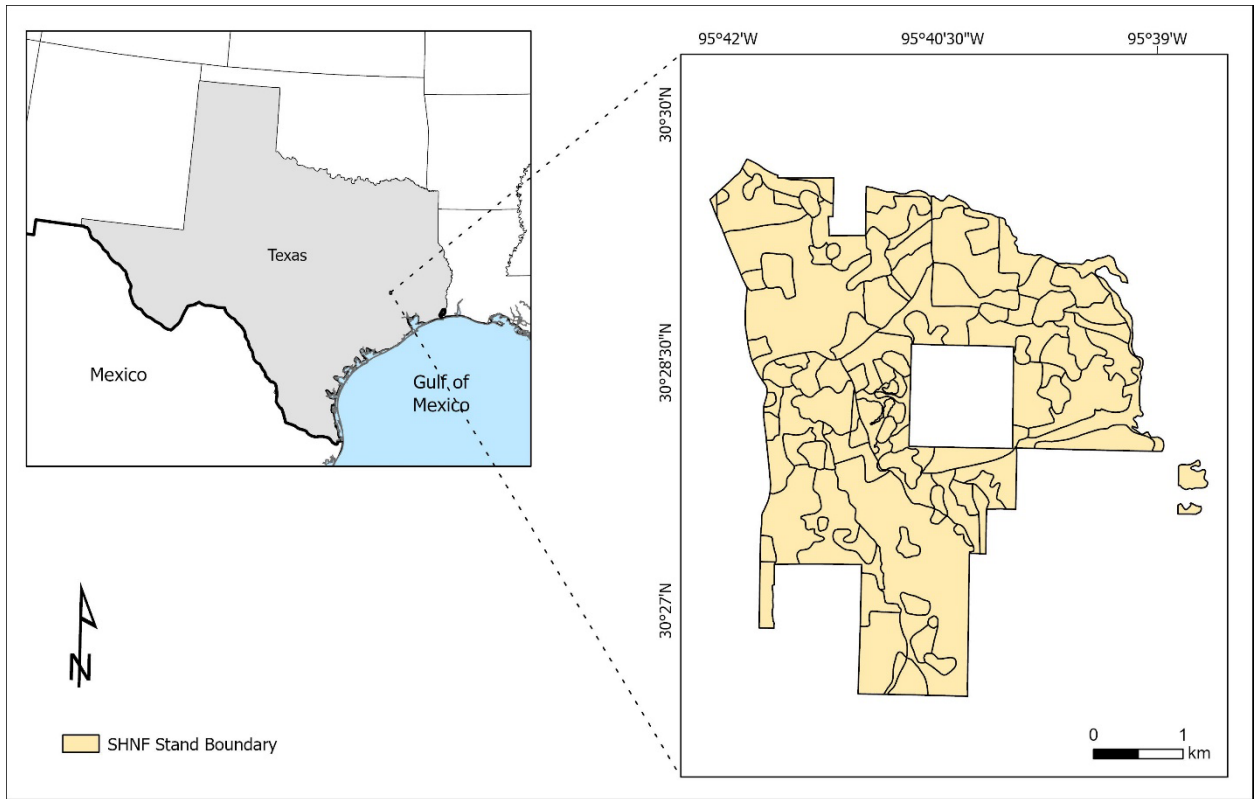
53 The acquisition of lidar on large scales is one example of a cost prohibitive approach to modeling
54 stand-level forest inventories, but open source lidar datasets create potential opportunities to conduct
55 analysis without incurring those costs. For this study, a 2018 USGS lidar dataset was collected two
56 years prior to a traditional forest inventory conducted on the Sam Houston National Forest in Walker
57 County, Texas, United States. I used this dataset to determine whether a geoprocessing workflow
58 could be developed for recreating stand-level volume, basal area (BA), and trees per acre (TPA) from
59 our Common Stand Exam (CSE) forest inventory. CSE inventory protocols were developed by, and

60 unique to the U.S. Forest Service. I also attempted to separately model shortleaf pine (*Pinus*
61 *echinata*) volume, which is a dominant overstory species but not as abundant as loblolly pine (*Pinus*
62 *taeda*) in most areas of our study site.

63 **Methods**

64 **2.1 Study area**

65 CSE data was collected in 105 stands within compartments 31-33 on the Sam Houston National
66 Forest (SHNF) in Spring 2020 (Figure 1). The SHNF is located in Walker, Montgomery, and San
67 Jacinto counties of Texas, United States, and is often characterized by mixed loblolly pine and
68 shortleaf pine overstory. The two can vary in their presence and abundance, with shortleaf pine being
69 an upland species and loblolly pine being a ubiquitous species. Major hardwood species include
70 southern red oak (*Quercus falcata*), post oak (*Quercus stellata*), cherrybark oak (*Quercus pagoda*),
71 American sweetgum (*Liquidambar styraciflua*), black tupelo (*Nyssa sylvatica*), and winged elm
72 (*Ulmus alata*). Hardwoods generally represent a small percentage of stand species composition
73 (<15%), with some exceptions on the east, northeast sides of the study site. Soils are mostly
74 characterized by fine sandy loams and loamy fine sands, with some areas of eroded and frequently
75 flooded clay soils to the northeast of the site.

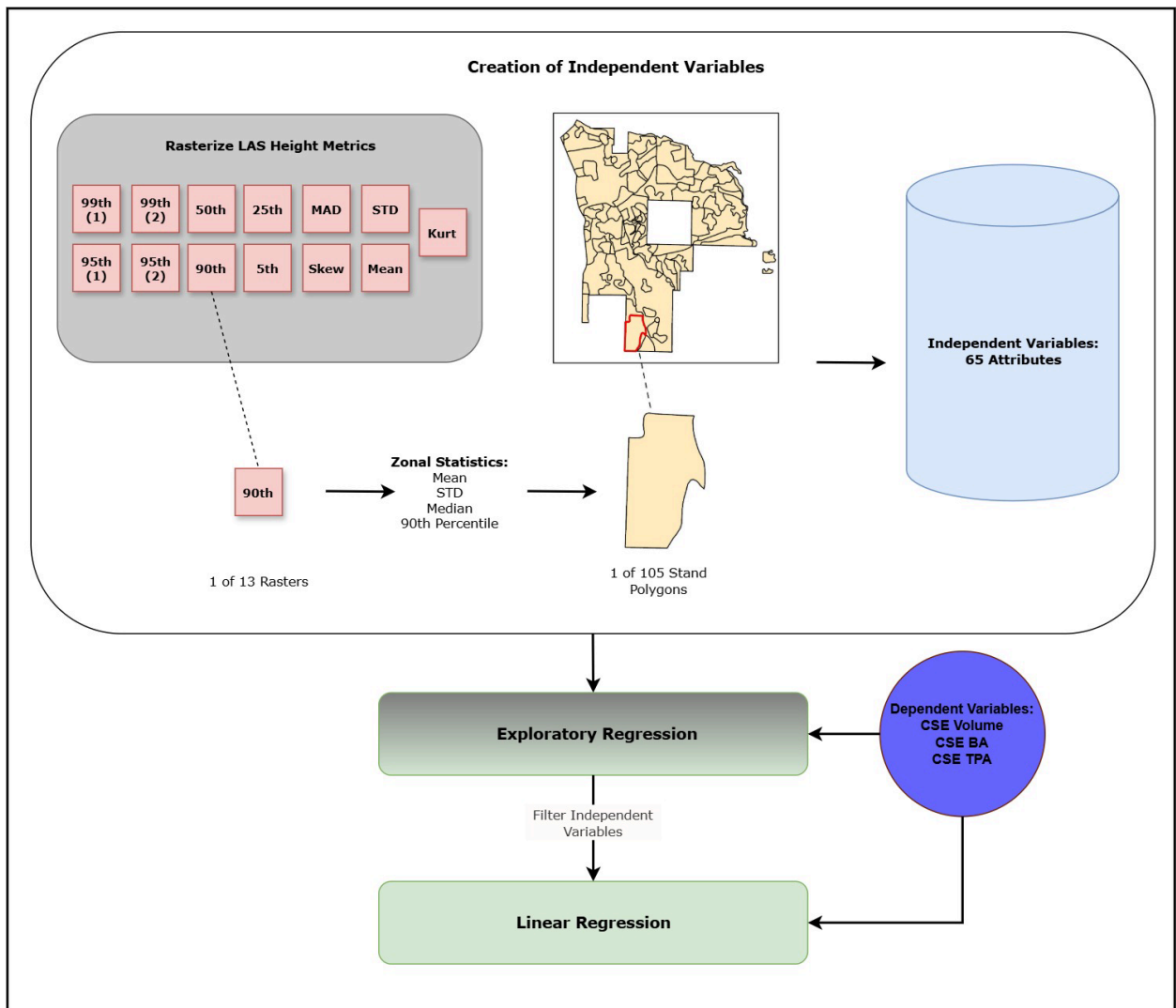


76

77 **Fig. 1.** Stands within Compartments 31-33 on the Sam Houston National Forest in Montgomery County,
78 Texas, United States. CSE data collected on the site in Spring of 2020.

79 **2.2 Workflow**

80 The workflow is broken into major steps that consist of creating independent variables from lidar
81 data, conducting an exploratory regression to filter independent variables, and using a small selection
82 of them to model linear relationships with dependent variables or CSE data (Figure 2). The Upper
83 Coast Lidar (UCL) dataset was used for my analysis and sourced from the Texas Natural Resources
84 Information System website (Texas Natural Resource Information System, 2018). Lidar data was
85 collected on January 13th, 2018 through March 22nd, 2018 during leaf-off conditions. UCL data was
86 acquired using a manned aircraft at a nominal point density of 4.37 pts/m² (Texas Water
87 Development Board, 2018).



88

89 **Fig. 2.** A workflow of how lidar data was rasterized into height metrics, and zonal statistics were
 90 generated for each stand in the study area. The resulting independent variables were filtered using an
 91 exploratory regression, and a small selection of them were used to model linear relationships with CSE
 92 inventory data (dependent variables).

93 UCL point cloud data was imported into ArcGIS Pro software (ESRI, Redlands, California, U.S.),
 94 and rasterized into thirteen different height metrics at 1 x 1 m pixel resolution. Each height metric
 95 rendered a raster layer where output pixels are a calculated value of their spatially coincident lidar
 96 points. Height metrics included: 99th and 95th percentile height points at a 10 m height minimum; 99th
 97 and 95th percentile height points at a 1 m height minimum, 90th percentile height points, 50th

98 percentile height points, 25th percentile height points, 5th percentile heights points, median absolute
99 distribution of height points, standard deviation (STD) of height points, kurtosis of height points,
100 skewness of height points, and mean of height points.

101 After rasterizing these 13 layers, I calculated zonal statistics for each in all 105 stands. For example,
102 the mean pixel value of 90th percentile heights were calculated within the area of each stand. Zonal
103 statistics included mean, STD, median, and 90th percentile of pixel values, and a total of 65 attributes
104 or independent variables were created. To filter out superfluous variables, I used exploratory
105 regression in ArcGIS Pro to determine which variables had the most significant relationship with
106 CSE metrics, the nature of their relationship (negative or positive), and eliminated redundant
107 variables that violated issues of multicollinearity. This drastically reduced the number of variables
108 that were later used when modeling linear relationships with CSE dependent variables.

109 ***2.3 Statistical Analysis***

110 A tabular format of stand level CSE results, and their corresponding lidar-derived variables were
111 exported from ArcGIS Pro and the remaining analysis performed in RStudio using R version
112 2024.04.2+764. Prior to performing any linear regression analysis, a Shapiro-Wilks test of normality
113 and Breusch-Pagan test of homoscedasticity was generated for each dependent and independent
114 variable pairing using the “rempsyc” package in R. Violations of either were noted later in results.

115 Using the most significant lidar-derived variable identified using exploratory regression, a linear
116 regression was performed modeling relationships with the following dependent variables: CSE stand-
117 level pine BA, pine TPA, hardwood BA, hardwood TPA, total BA, pine merchantable volume, pine
118 board ft volume, merchantable volume of loblolly pine, board ft volume of loblolly pine, and
119 merchantable volume of shortleaf pine. All my analysis was performed at a 95th confidence interval.

120 Results

121 3.1 Linear Regression: BA and TPA

122 Lidar-derived independent variables maintained a statistically significant relationship with stand-

123 level CSE measurements of BA and TPA, but did not explain the variation well when modeling

124 linear relationships ($R^2 < 0.4$). Both hardwood and pine groups had examples of independent

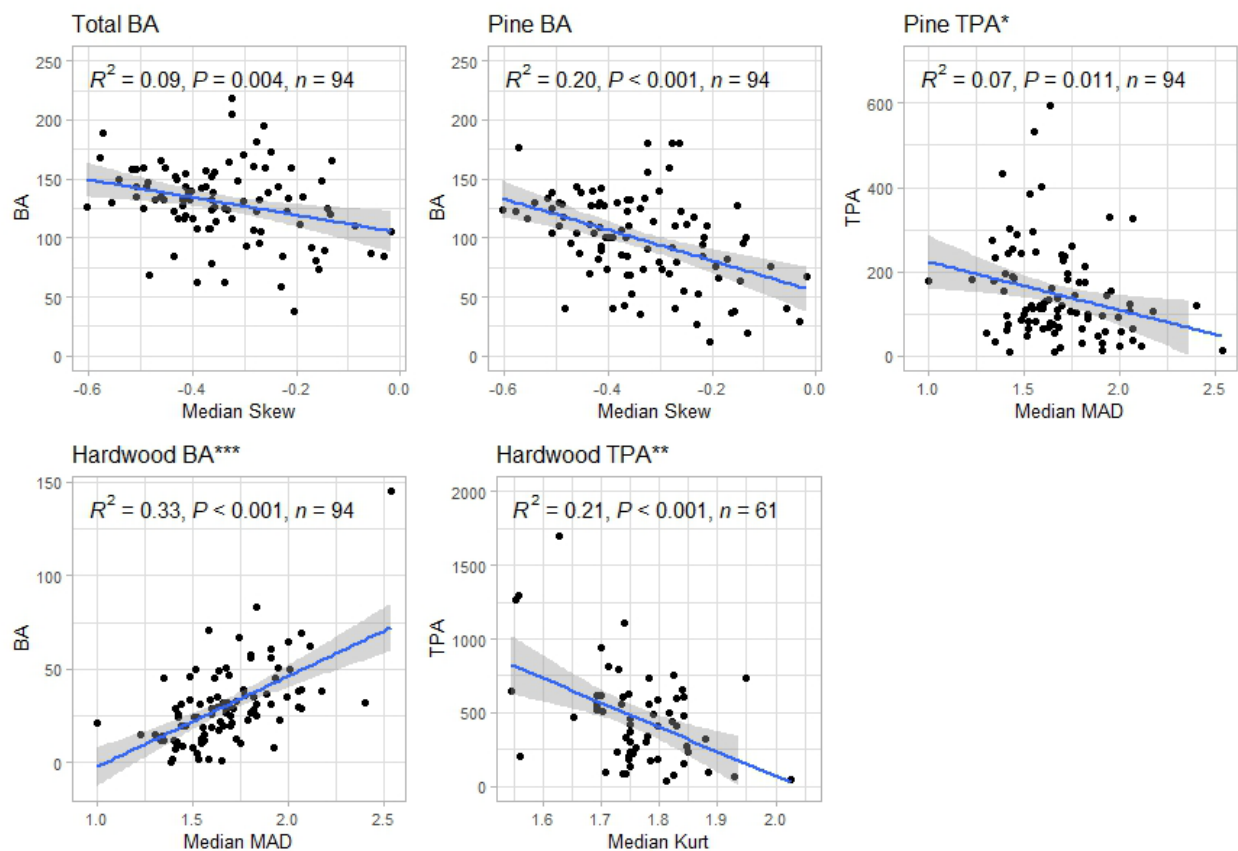
125 variables that uniquely maintained significant relationships with BA and TPA, except for median

126 MAD, which had a statistically significant relationship with both pine TPA and hardwood BA.

127 Median zonal statistics were consistently the strongest independent variable for modeling linear

128 relationships with BA and TPA metrics, including median skew, median MAD, and median kurtosis

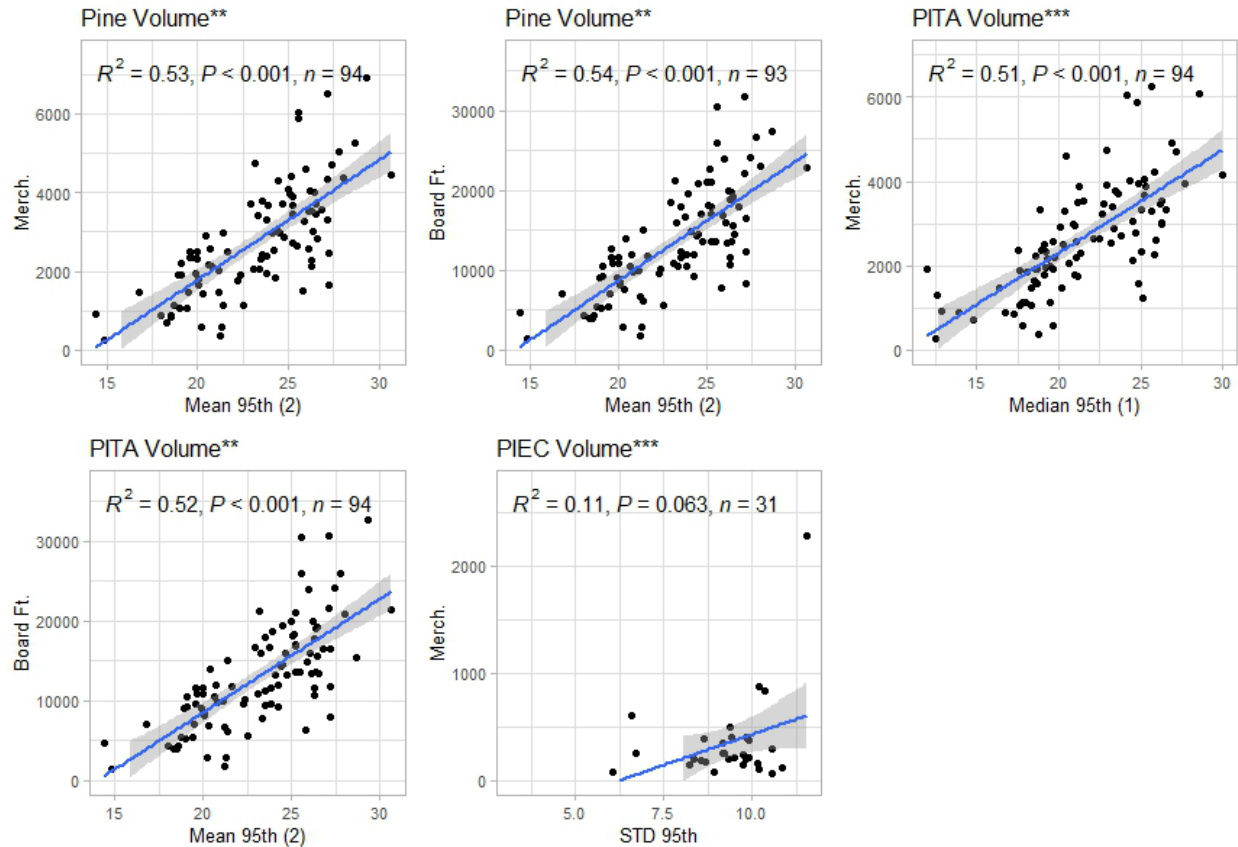
129 (Figure 3).



131 **Fig. 3.** Linear regression results for Total BA, Pine BA and TPA, and Hardwood BA and TPA. CSE data
132 was used for dependent variables and lidar data was processed into independent variables. Violated
133 assumptions of normality*, homoscedasticity**, and both*** are noted.

134 ***3.2 Linear Regression: Volume***

135 Compared to linear modeling of BA and TPA, merchantable and board ft volume exhibited stronger
136 relationships with certain lidar-derived independent variables. For all pine and loblolly pine volumes
137 (merchantable and board ft), dependent variables demonstrated a statistically significant relationship
138 with mean 95th percentile zonal statistics (Figure 4). These linear relationships explained relatively
139 more of the variation in the dependent variable, with an R^2 of 0.5 or greater. STD 95th percentile
140 zonal statistics was the strongest variable for modeling relationships with shortleaf pine volume
141 during exploratory regression, but did not demonstrate a statistically significant relationship when
142 performing linear regression ($p = 0.063$). It did however maintain a near statistically significant
143 relationship, and notably, with an independent variable that was different from loblolly pine.



144

145 **Fig. 4.** Linear regression results for all pine merchantable and board ft. volume, loblolly pine (PITA)
146 merchantable and board ft. volume, and shortleaf pine (PIEC) merchantable volume. CSE data was used
147 for dependent variables and lidar data was processed into independent variables. Violated assumptions of
148 normality*, homoscedasticity**, and both*** are noted.

149

150 Discussion & Conclusion

151 The results of my analysis indicate that open sourced lidar can be processed into explanatory
152 variables that have the potential to model simple, linear relationships with traditionally collected CSE
153 data. For BA and TPA CSE metrics, there were inherent weaknesses in my analysis, such as low
154 explanation of variation, and violations of assumptions in linear regression. Despite statistically

155 significant results when analyzing BA and TPA, this would make it unlikely that my current methods
156 could be used to extrapolate reliable predictions of BA or TPA. More refined modeling techniques
157 applied in similar scenarios, including data fusion (Popescu and Wynne, 2004; Lawrence, 2024) and
158 deep learning (Mäyrä et al., 2021; Klauberg et al., 2023), might be potential avenues for improving
159 the predictive capabilities of such models.

160 Linear relationships of lidar-derived variables and volume were stronger and showed potential to
161 possess predictive capabilities. This indicates that these methods could successfully circumvent
162 traditional field inventories where volume is an important consideration, although it is unlikely to be
163 the only information necessary for informing management decisions. It was also of interest to
164 determine whether shortleaf pine volume could specifically be modeled, because of its relatively low
165 abundance compared to loblolly pine. Despite near significant results, we were unable to identify a
166 lidar-derived variables that individually maintained a statistically significant relationship with
167 shortleaf pine volume.

168 Similar studies have leveraged open-sourced Landsat and Sentinel 2 data to classify canopy coverage
169 of southern yellow pine, including shortleaf pine and loblolly pine (Akumu and Amadi, 2022). In this
170 example, canopy cover, and possibly stand-level species composition, might be determined. In other
171 examples, hyperspectral data was used to investigate whether spectral characteristics specific to each
172 southern yellow pine species could be distinguished using field-based (van Aardt, 2000) and remote
173 sensing methods (Van Aardt and Wynn, 2007). Again, data fusion, and in particular non-visible light
174 spectra generated from multispectral or hyperspectral sensors, are potential datasets that could
175 increase the likelihood of successfully modeling shortleaf versus loblolly pine volume in future work.
176 Ultimately, this study demonstrates that open-sourced lidar data is a potential means for recreating
177 CSE metrics, some of which maintain a strong enough relationship to make predictions of nearby and
178 similar stand volume. This could translate to significant cost reductions and efficiencies, in the event

179 traditional, personnel-intensive forest inventories could be augmented or replaced by remote sensing
180 methods. Refinements of methodology, in particular fusing our lidar raster data with non-visible
181 spectral data, could be one approach to modeling more accurate relationships with other CSE metrics
182 like BA, TPA, and maybe even species-specific metrics.

183 **Declarations**

184 **Ethics approval and consent to participate:** Not applicable

185 **Consent for publication:** Not applicable

186 **Availability of data and material:** Data can be made upon reasonable request to the corresponding
187 author.

188 **Competing interests:** The author declares that they have no competing interests.

189 **Funding:** This research received no external funding.

190 **Authors' contributions:** BL: conceptualization, data curation, formal analysis, methodology,
191 validation, writing - original draft, and writing - review and editing.

192 **Acknowledgements:** The author thanks Kerry Hogg of the U.S. Forest Service for providing
193 stocking and volume reports of the site and permitting the use of the data for the study. I also want to
194 thank the Sam Houston National Forest staff for the opportunity to use the forest as a study site.

195 **References**

- 196 1. Akumu, C.E., Amadi, E.O., 2022. Examining the Integration of Landsat Operational Land
197 Imager with Sentinel-1 and Vegetation Indices in Mapping Southern Yellow Pines (Loblolly,
198 Shortleaf, and Virginia Pines). *photogramm eng remote sensing* 88, 29–38.
199 <https://doi.org/10.14358/PERS.21-00024R2>
- 200 2. Anderson, C.T., Dietz, S.L., Pokswinski, S.M., Jenkins, A.M., Kaeser, M.J., Hiers, J.K., Pelc,
201 B.D., 2021. Traditional field metrics and terrestrial LiDAR predict plant richness in southern
202 pine forests. *Forest Ecology and Management* 491, 119118.
203 <https://doi.org/10.1016/j.foreco.2021.119118>
- 204 3. Balestra, M., Marselis, S., Sankey, T.T., Cabo, C., Liang, X., Mokroš, M., Peng, X., Singh,
205 A., Stereńczak, K., Vega, C., Vincent, G., Hollaus, M., 2024. LiDAR Data Fusion to Improve
206 Forest Attribute Estimates: A Review. *Curr. For. Rep.* 10, 281–297.
207 <https://doi.org/10.1007/s40725-024-00223-7>
- 208 4. Brosofske, K.D., Froese, R.E., Falkowski, M.J., Banskota, A., 2014. A Review of Methods
209 for Mapping and Prediction of Inventory Attributes for Operational Forest Management.
210 *Forest Science* 60, 733–756. <https://doi.org/10.5849/forsci.12-134>
- 211 5. Dubayah, R., Drake, J., 2000. Lidar Remote Sensing for Forestry. *Journal of Forestry* 98, 44–
212 46. <https://doi.org/10.1093/jof/98.6.44>
- 213 6. Hemingway, H., Opalach, D., 2024. Integrating Lidar Canopy Height Models with Satellite-
214 Assisted Inventory Methods: A Comparison of Inventory Estimates. *Forest Science* 70, 2–13.
215 <https://doi.org/10.1093/forsci/fxad047>
- 216 7. Hummel, S., Hudak, A.T., Uebler, E.H., Falkowski, M.J., Megown, K.A., 2011. A
217 Comparison of Accuracy and Cost of LiDAR versus Stand Exam Data for Landscape
218 Management on the Malheur National Forest. *Journal of Forestry* 109, 267–273.
219 <https://doi.org/10.1093/jof/109.5.267>

- 220 8. Klauberg, C., Vogel, J., Dalagnol, R., Ferreira, M.P., Hamamura, C., Broadbent, E., Silva,
221 C.A., 2023. Post-Hurricane Damage Severity Classification at the Individual Tree Level
222 Using Terrestrial Laser Scanning and Deep Learning. *Remote Sensing* 15, 1165.
223 <https://doi.org/10.3390/rs15041165>
- 224 9. Lawrence, B., 2024. Lidar-based MaxEnt models to support conservation planning for
225 endangered Red-cockaded Woodpeckers in urbanizing environments. *Remote Sensing*
226 *Applications: Society and Environment* 34, 101190.
227 <https://doi.org/10.1016/j.rsase.2024.101190>
- 228 10. Mäyrä, J., Keski-Saari, S., Kivinen, S., Tanhuanpää, T., Hurskainen, P., Kullberg, P.,
229 Poikolainen, L., Viinikka, A., Tuominen, S., Kumpula, T., Vihervaara, P., 2021. Tree species
230 classification from airborne hyperspectral and LiDAR data using 3D convolutional neural
231 networks. *Remote Sensing of Environment* 256, 112322.
232 <https://doi.org/10.1016/j.rse.2021.112322>
- 233 11. Popescu, S.C., Wynne, R.H., 2004. Seeing the Trees in the Forest: Using Lidar and
234 Multispectral Data Fusion with Local Filtering and Variable Window Size for Estimating
235 Tree Height. *photogramm eng remote sensing* 70, 589–604.
236 <https://doi.org/10.14358/PERS.70.5.589>
- 237 12. Ross, C.W., Loudermilk, E.L., O'Brien, J.J., Flanagan, S.A., McDaniel, J., Aubrey, D.P.,
238 Lowe, T., Hiers, J.K., Skowronski, N.S., 2024. Lidar-derived estimates of forest structure in
239 response to fire frequency. *fire ecol* 20, 44. <https://doi.org/10.1186/s42408-024-00279-7>
- 240 13. Sumnall, M.J., Trlica, A., Carter, D.R., Cook, R.L., Schulte, M.L., Campoe, O.C., Rubilar,
241 R.A., Wynne, R.H., Thomas, V.A., 2021. Estimating the overstory and understory vertical
242 extents and their leaf area index in intensively managed loblolly pine (*Pinus taeda* L.)
243 plantations using airborne laser scanning. *Remote Sensing of Environment* 254, 112250.
244 <https://doi.org/10.1016/j.rse.2020.112250>

- 245 14. Texas Natural Resource Information System (TNRIS), 2018. Strategic Mapping Program
246 (Stratmap). Upper Coast Lidar. Available at <https://tnris.org/stratmap/elevation-lidar/>
247 (Accessed on 15 October 2022)
- 248 15. Texas Water Development Board (TWDB), 2018. 2018 Coastal Texas Lidar Final QA/QC
249 Report. Available at [https://prd-
250 tnm.s3.amazonaws.com/StagedProducts/Elevation/metadata/TX_CoastalRegion_2018_A18/
251 TX_Coastal_B1_2018/reports/thrid-party-](https://prd-tnm.s3.amazonaws.com/StagedProducts/Elevation/metadata/TX_CoastalRegion_2018_A18/TX_Coastal_B1_2018/reports/thrid-party-)
- 252 16. van Aardt, J.A.N, 2000. Spectral Separability among Six Southern Tree Species (Master of
253 Science in Forestry). Virginia Polytechnic Institute and State University, Blacksburg, VA.
- 254 17. Van Aardt, J.A.N., Wynne, R.H., 2007. Examining pine spectral separability using
255 hyperspectral data from an airborne sensor: An extension of field-based results. *International
256 Journal of Remote Sensing* 28, 431–436. <https://doi.org/10.1080/01431160500444772>
- 257 18. Wu, J., Man, Q., Yang, X., Dong, P., Ma, X., Liu, C., Han, C., 2024. Fine Classification of
258 Urban Tree Species Based on UAV-Based RGB Imagery and LiDAR Data. *Forests* 15, 390.
259 <https://doi.org/10.3390/f15020390>